

## PAPER



Cite this: *J. Anal. At. Spectrom.*, 2022, **37**, 1259

## Steady analyses of potassium stable isotopes using a Thermo Scientific Neoma MC-ICP-MS†

Philippe Télouk,<sup>a</sup> Emmanuelle Albalat,<sup>a</sup> Théo Tacail,<sup>b</sup> Florent Arnaud-Godet<sup>a</sup> and Vincent Balter \*<sup>a</sup>

Potassium stable isotope compositions (<sup>41</sup>K/<sup>39</sup>K ratio) exhibit a wide range of natural variation (~3‰), whose measurement has been recently achievable thanks to the development of various methods, including collision cell, XHR mode, cold and dry plasma, or dummy bucket MC-ICP-MS. Here, we report the capabilities of a Thermo Scientific new generation MC-ICP-MS, Neoma, to routinely measure the <sup>41</sup>K/<sup>39</sup>K ratio. We found that the effect of potassium concentration mismatch between the sample and standard is comparable to other reported methods. However, the effect of acid concentration mismatch is not perceptible from 0.05 M to 0.5 M HNO<sub>3</sub>, and the effect of matrix elements on the accuracy of sample-standard bracketing measurements is lower compared to other reported methods up to the element-K normalized ratio of >15%. This relative insensibility to non-spectral matrix effects most probably results from the new design of the introduction system that integrates an iCAP Qnova Series ICP-MS torch and injector assembly. The resulting repeatability (or short-term external precision) and long-term intermediate precision (or long-term reproducibility) are 0.06‰ (2SD, *n* = 55) and 0.07‰ (2SD, *n* = 12), respectively. We then use a very simple one step chemical purification of K by ion exchange chromatography and apply the method to the measurement of the δ<sup>41</sup>K value of geological and biological reference materials, and blood samples of cancer and control patients. The results for reference materials show very good agreement with previously reported values and extend the available data for future interlaboratory comparison studies. Blood samples of cancer and control patients exhibit similar δ<sup>41</sup>K values despite a suspected isotopic difference between tumour and normal tissues. The overall instrumental robustness observed using the XHR mode remains to be challenged with the precell mass filter and hexapole collision/reaction cell upgrade.

Received 18th February 2022  
Accepted 12th April 2022

DOI: 10.1039/d2ja00050d

rsc.li/jaas

## Introduction

Potassium has two stable isotopes, <sup>39</sup>K (93.2581%) and <sup>41</sup>K (6.7302%). Similarly to D/H, the <sup>41</sup>K/<sup>39</sup>K ratio has been suspected in the 1930s to be variable due to so-called physiological isotope effects.<sup>1,2</sup> These primitive measurements of the <sup>41</sup>K/<sup>39</sup>K ratio were associated with large uncertainties which have been reduced down to hundreds of ppm only after eighty years thanks to the development of multicollector ICP-MS (MC-ICP-MS). However, the challenge in the measurement of the <sup>41</sup>K/<sup>39</sup>K ratio by MC-ICP-MS is that argides are produced in the Ar plasma, with significant isobaric interferences of <sup>40</sup>ArH<sup>+</sup> on <sup>41</sup>K<sup>+</sup>, and less importantly of <sup>38</sup>ArH<sup>+</sup> on <sup>39</sup>K<sup>+</sup>. Three main solutions have been developed to drastically reduce these interferences to achieve an external precision ≤0.2‰ of the δ<sup>41</sup>K value.

The first solution is to use cold and dry Ar plasma<sup>3-7</sup> with a potential additional dummy bucket to collect <sup>40</sup>ArH<sup>+</sup>.<sup>8</sup> The idea of cooling the plasma temperature dates back to the 1990s<sup>9</sup> and consists of drastically reducing the ionization efficiency of Ar (15.76 eV) while keeping that of K (4.34 eV) less affected. In addition, the use of a desolvating system decreases H<sub>2</sub>O-based interferences by removing solvent vapours. However, these instrumental settings generally lead to unstable conditions due to the very narrow (0.002–0.004 amu) <sup>40</sup>ArH<sup>+</sup> interference-free flat shoulder where the <sup>41</sup>K<sup>+</sup> beam is measured. As a consequence, cold and dry Ar plasma conditions are often associated with significant matrix effects.<sup>4,7</sup>

The second solution is offered by MC-ICP-MS instruments equipped with a collision/reaction cell (CC), whose goal is to eliminate isobaric interferences *via* collision and reaction in an axial chamber filled with a reactive gas. While the CC technology is now integrated into most commercially available quadrupole-based ICP-MS instruments, its combination with multiple collection is very recent. A first attempt of CC integration into a single-focusing MC-ICP-MS (GV Instruments, Manchester, UK) was commercialized in the 2000s with the

<sup>a</sup>Université de Lyon, Ecole Normale Supérieure de Lyon, Université de Lyon 1, CNRS, LGL-TPE, Lyon, France. E-mail: Vincent.Balter@ens-lyon.fr

<sup>b</sup>Institute of Geosciences, Johannes Gutenberg University, Mainz, Germany

† Electronic supplementary information (ESI) available. See <https://doi.org/10.1039/d2ja00050d>

IsoProbe-P. The measurement of the  $^{41}\text{K}/^{39}\text{K}$  with this instrument is generally associated with an external precision of about 0.2‰ (2SD), which is unsatisfactory for resolving small  $\delta^{41}\text{K}$  variations.<sup>10–12</sup> The 2020s have seen the commercialization of the Sapphire (Nu Instruments, Wrexham, UK), a dual-path CC-MC-ICP-MS allowing an external reproducibility of about 0.05‰ for routine measurements of the  $^{41}\text{K}/^{39}\text{K}$  ratio at  $\sim 150$  ppb.<sup>13–15</sup> During this period, Thermo Scientific (Bremen, Germany) developed the Proteus MC-ICP-MS, in which the ICP module of the iCAP-Q replaces the original ICP module of the Neptune Plus.<sup>16</sup> However, the Proteus suffers from low sensitivity and unusual mass bias behavior, and the iCAP-Q module was replaced by a new module containing two Wien filters and a hexapole, leading to the Vienna prototype,<sup>17</sup> which was not commercialized.

The third solution is to take advantage of the extra-high resolution mode (XHR) of the Neptune XT (Thermo Scientific, Bremen, Germany) MC-ICP-MS. The XHR option allows the improvement of the existing high resolution (25  $\mu\text{m}$  wide slit) to an extra-high resolution using an additional 16  $\mu\text{m}$  wide slit installed after the electrostatic analyzer that can be switched in and out of position using a pneumatic control. Regarding K isotopes, the resolution increases from 9000 to 15 000, leading to precise and accurate measurements of the  $^{41}\text{K}/^{39}\text{K}$  ratio.<sup>18</sup> A table summarizing all the compared setups and the corresponding general performances is provided as Table S1.†

Here, we measure the  $^{41}\text{K}/^{39}\text{K}$  ratio using a Neoma MC-ICP-MS, which has been commercialized by Thermo Scientific in 2020. The Neoma is a pseudo-high resolution MC-ICP-MS, whose design is based on that of the Neptune XT with many new features, notably the detection system which now includes 11 independent Faraday cups connected to 24 amplifier slots. For the interest of the present paper, it is noteworthy that the sample introduction assembly has been replaced by that of an iCAP RQ/TQ ICP-MS (iCAP Qnova Series ICP-MS). This instrument can be upgraded to a Neoma MS/MS version with a reaction and collision cell before entering the ESA with prefiltering of the ions through a double Wien filter.<sup>17</sup> In the MS/MS mode, the XHR mode is no longer needed, and the full transmission in low resolution mode will be used. We show that the Neoma is markedly insensitive to matrix effects and allows a single step K purification for accurate measurements of the  $^{41}\text{K}/^{39}\text{K}$  ratio in biological samples. Accuracy of the  $^{41}\text{K}/^{39}\text{K}$  ratio is demonstrated by measuring several geological and biological reference materials. We also report the serum  $^{41}\text{K}/^{39}\text{K}$  ratio of acute myeloid leukemia patients and control participants with the aim of evaluating the potential of K isotope composition as a diagnostic biomarker.

## Materials

### Reagents and materials

All experiments were carried out in laminar flow hoods in a clean laboratory. Acids ( $\text{HNO}_3$ ,  $\text{HCl}$ , and  $\text{HF}$ ) were double-distilled to reduce blank contaminations. Suprapur 30%  $\text{H}_2\text{O}_2$  (Fisher Chemical, Hampton, NH, USA) was used. Ultrapure water (resistivity > 18.2  $\text{M}\Omega\text{ cm}$ ) was obtained from a Milli-Q

Element water purification system (Merck Millipore, Bedford, MA, USA). Teflon® columns (custom-made using retractable Teflon) filled with 210  $\mu\text{L}$  of AG50W-X12 resin, hydrogen form 200–400 mesh size, purchased from Bio-Rad (Temse, Belgium) were used for K purification. Teflon beakers (Savillex™, Eden Prairie, MN, USA) were used throughout the procedure, from digestion to ultimate dilution.

### Sample description

We used the GA (CRPG, Nancy, France) granite and BHVO-2 (USGS) and BCR-1 (USGS) basalts for geological reference materials, the IAPSO (OSIL) certified reference seawater standard, and the bovine liver SRM-1577c (NIST), green beans BCR-383 (NRC), rye grass (ERM-CD 281), whole milk BCR-380R (NRC), tuna fish ERM-CE 464 (IRMM), fish protein DORM-4 (NRC), lobster hepatopancreas TORT-3 (NRC), fetal bovine serum FBS (Sigma-Aldrich, lot number 014M3399) and in-house human plasma pooled from several samples, for biological reference materials. Blood serum samples were collected from control participants ( $n = 10$ ) and patients ( $n = 9$ ) with newly diagnosed acute myeloid leukemia presented to Hospices Civils de Lyon, from January 2015 to April 2016.<sup>19</sup> The analysis of samples was approved by the Institutional Review Board of Hospices Civils de Lyon, Centre de Protection des Personnes du Centre Léon Bérard, ENS-Lyon, and the French Government Ministry of Health. Control samples, with the same age range as patients, were obtained from blood donors at Etablissement Français du Sang during the same time.

## Methods

### Sample digestion

A minimum sample size of 100 mg was weighed for reference materials to avoid measurement uncertainties due to the heterogeneity of the reference material powder. Geological reference materials were digested with a mixture of 5 mL of 27 M distilled HF and 2.5 mL of 15 M distilled  $\text{HNO}_3$  at 120 °C for 12 hours and evaporated to dryness. Fluorides were further dissolved using 2 mL of 6 M  $\text{HCl}$  and heated on a hotplate at 100 °C for 12 hours and then evaporated to dryness. Biological reference materials were digested in clean PTFE microwave bombs using 4 mL of concentrated distilled  $\text{HNO}_3$  and 1 mL of Suprapur 30%  $\text{H}_2\text{O}_2$ . The bombs were then sealed and placed in a Milestone Ethos microwave (Milestone, Sorisole, Italy) set to ramp up to 180 °C in 20 min and remain at 180 °C for 40 min. The solutions were then evaporated to dryness on a hot plate at 90 °C in Teflon® beakers.

### K purification

The K purification is achieved using ion-exchange chromatography with a protocol based on Mg purification.<sup>20</sup> For biological reference materials and blood samples, a one-step procedure corresponding to the third purification step of Le Goff *et al.*<sup>20</sup> is utilized for K purification (Table 1).

For mafic reference materials (BHVO-2 and BCR-1 basalts), a second step was necessary to further purify K from the matrix,

**Table 1** Ion exchange protocol for the chromatographic separation of K

AG50W-X12 (200–400 mesh), $V = 0.21$ mL, diam = 0.42 cm stored in $H_2O$	
<b>Rinsing</b>	
6 M HCl	4 mL
$H_2O$	4 mL
6 M HCl	8 mL
<b>Conditioning</b>	
0.4 M HCl	2.5 mL
<b>Loading</b>	
0.4 M HCl	0.25 mL
<b>Matrix elution</b>	
0.4 M HCl	5 mL
<b>K elution</b>	
0.4 M HCl	8 mL

**Table 2** Instrument settings for K isotope analysis

Neoma MC-ICP-MS	
RF power (W)	1200
Plasma condition	Wet, quartz cyclonic/ Scott double spray chamber
Coolant Ar flow ( $L\ min^{-1}$ )	15
Auxiliary Ar flow ( $L\ min^{-1}$ )	0.8–1.1
Mass resolution	>15 000 (XHR mode)
Sampling cone	Ni jet, $\phi = 1.1$ mm
Skimmer cone	Ni H-type, $\phi = 0.8$ mm
Cup configuration	H4: $^{44}Ca$ ; H3: $^{43}Ca$ ; H1: $^{42}Ca$ ; Ax: $^{41}K$ ; L1: $^{39}K$ ; L3: $^{38}Ar$
Sensitivity ( $V\ ppm^{-1}$ )	$\sim 40$
Blank signal (2% $HNO_3$ )	$^{39}K \sim 10$ mV
Integration time (s)	4.194
Cycles	40
<b>Aridus II desolvator</b>	
Ar flow ( $L\ min^{-1}$ )	9.8
$N_2$ flow ( $mL\ min^{-1}$ )	6
Sample uptake rate ( $\mu L\ min^{-1}$ )	100

which was used by several authors,<sup>3,7,15</sup> and initially set up by Strelow *et al.*<sup>21</sup> Briefly, Bio-Rad columns were filled with 2 mL of AG50W-X8 resin and conditioned with 10 mL  $HNO_3$  (0.5 M). Matrix elements were eluted with 13 mL of  $HNO_3$  (0.5 M), and K was collected from the subsequent 22 mL fraction.

### K isotope ratio measurements

All the measurements in this study were conducted on a Neoma MC-ICP-MS at the LGL (Laboratoire de Géologie de Lyon, Ecole Normale Supérieure de Lyon, France) using a hot plasma, the XHR option and an Aridus II desolvator system (Teledyne CETAC Technologies Inc., NE, USA), with a PFA nebulizer,



**Fig. 1** Peak scan of the SRM-3141a solution at  $1\ mg\ L^{-1}$  using the set of parameters given in Table 2 showing the peak shape of the  $m/z$  value 39 (yellow) with the automated calculation of the resolution (5, 95% of  $m/z$  value 39) on the ascending edge of the peak. Potassium isotope ratio measurement was performed at the middle of the  $^{40}ArH^+$  interference-free plateau of the  $^{41}K^+$  peak. The software used is an adapted version of Qtegra for MC-ICP-MS analysis.

according to instrument parameters given in Table 2. The measurement of the K isotope ratio was performed on a flat and free of interference mass range of  $\sim 0.005$  amu (Fig. 1) using the Faraday cup configuration as given in Table 2.

Given this set of parameters, a K solution at  $1\ mg\ L^{-1}$  gives a typical  $^{39}K$  voltage of  $\sim 40$  V, which is about two-thirds more sensitive than with a Neptune XT.<sup>18</sup> The sample-standard bracketing approach with a solution of SRM-3141a (NIST) as the external standard is then used for correcting instrumental mass discrimination. Analyses are carried out using 0.05 M  $HNO_3$  with blank correction (on-peak zero) before measurement and the K isotopic composition is expressed as a delta value ( $\delta^{41}K$ , per mil, ‰) relative to SRM-3141a according to:

$$\delta^{41}K = \left[ \frac{(^{41}K/^{39}K)_{\text{sample}}}{(^{41}K/^{39}K)_{\text{standard}}} - 1 \right] \times 1000$$

## Results and discussion

Prior to the measurement of the K isotope ratio in reference materials or natural samples, it is necessary to evaluate the influence of several analytical conditions on the precision and accuracy of the sample-standard bracketing measurements. An acid blank of 0.05 M  $HNO_3$  typically yields a  $^{39}K$  signal of 13 mV ( $\sim 1$  mV for  $^{41}K$ ), which represents a negligible contribution of  $\sim 0.03\%$  compared to a sample measured at  $1\ mg\ L^{-1}$  ( $\sim 40$  V for  $^{39}K$  and  $\sim 3.1$  V for  $^{41}K$ ).

### Effect of K concentration mismatch on the $^{41}K/^{39}K$ ratio

When using the sample-standard bracketing method, concentration mismatch between samples and standards, as for other elements (*e.g.* ref. 22), could have a strong effect on the  $\delta^{41}K$

value of the sample, which is particularly true under cold plasma conditions. Following the precaution adopted by most of the papers reporting  $^{41}\text{K}/^{39}\text{K}$  ratio analyses, we have evaluated the influence of the K concentration mismatch between the sample and standard. Briefly, the SRM-3141a solution was diluted at varying concentrations to obtain a  $[\text{K}]_{\text{standard}}/[\text{K}]_{\text{sample}}$  between 0.8 and 1.4. The results are compared to the literature values and shown in Fig. 2.

The results generally show a decreasing  $\delta^{41}\text{K}$  value with increasing K concentration mismatch, except for the study of Gu *et al.*<sup>4</sup> in which the  $^{41}\text{K}/^{39}\text{K}$  ratio is measured using a Neptune + under cold plasma and low-resolution conditions. Our results show a weaker dependency to K concentration mismatch compared to CC-MC-ICP-MS,<sup>13,15</sup> but a higher dependency compared to a dummy bucket- or XHR-equipped MC-ICP-MS<sup>8,18</sup> (Fig. 2). The significant sensitivity of CC-MC-ICP-MS to concentration mismatch is well explained by the fact that the  $^{41}\text{K}/^{39}\text{K}$  ratio is measured at 150 ppb, whereas non-CC-equipped MC-ICP-MS necessitates much more analyte to be measured accordingly ( $\leq 1$  ppm). It is worth noting that Hu *et al.*<sup>5</sup> report  $^{41}\text{K}/^{39}\text{K}$  ratios free of K concentration mismatch effects despite measurements using a Nu Plasma II under cold plasma and low-resolution conditions.

### Effect of acid molarity mismatch on the $^{41}\text{K}/^{39}\text{K}$ ratio

When using the sample-standard bracketing method, the mismatch in the acid concentration between samples and standards also has a potential effect on the  $\delta^{41}\text{K}$  value of the sample.<sup>4,8,13,15,18</sup> Under the working conditions of the present study, the molarity of  $\text{HNO}_3$  is 0.05 M and we have evaluated the influence of the mismatch of the acid concentration from 0.025 M to 0.5 M and compared the results with the literature values (Fig. 3).

The results show good stability of the  $\delta^{41}\text{K}$  value, which does not offset significantly from 0‰ (Fig. 3). Cold plasma conditions<sup>4,8</sup> are particularly sensitive to the mismatch of the acid concentration between samples and standards. Cold

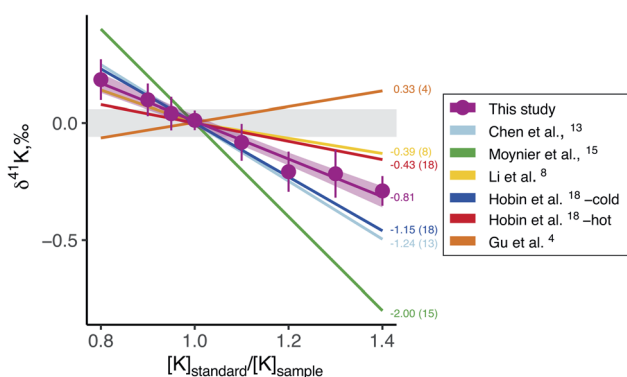


Fig. 2 Effect of K concentration mismatch between the sample and standard on the  $\delta^{41}\text{K}$  value of the sample. The slope of the regression lines, which has been determined graphically, is indicated for each contribution. The numbers in brackets are for the corresponding references. The gray area represents  $\pm 0.07\text{‰}$  from SRM-3141a. The error bars are  $\pm 2\text{SD}$ .

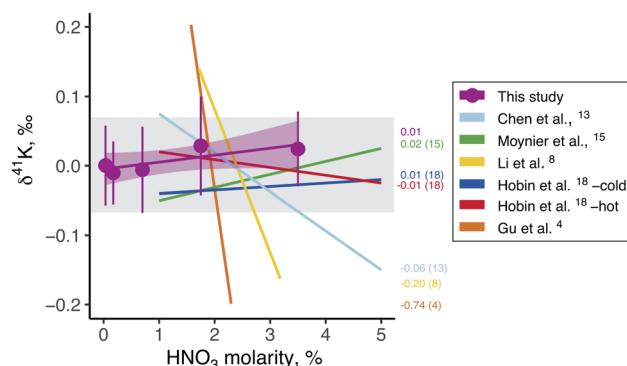


Fig. 3 Effect of mismatch of the acid concentration between samples and standards on the  $\delta^{41}\text{K}$  value of the sample. The slope of the regression lines, which has been determined graphically, is indicated for each contribution. The numbers in brackets are for the corresponding references. The gray area represents  $\pm 0.07\text{‰}$  from SRM-3141a. The error bars are  $\pm 2\text{SD}$ .

temperature causes the background mass spectrum to become dominated by  $\text{NO}^+$ ,<sup>9</sup> which combined with the varying  $\text{HNO}_3$  concentration most probably generates very different plasma conditions between the sample and standard. A possible way to overcome this problem is to use dilute  $\text{HCl}$  instead of  $\text{HNO}_3$ .

### Matrix effects on the $^{41}\text{K}/^{39}\text{K}$ ratio

The MC-ICP-MS routine measurement of isotope ratio necessitates the isolation of the analyte using ion-exchange chromatography. However, the yield of ion-exchange can vary from sample to sample, leading to incomplete analyte purification which generally causes non-spectral matrix effects, also known as matrix induced signal intensity changes,<sup>23</sup> due to ionization and transmission disturbance of the analyte. Since the discovery of the interest of cold plasma conditions for the measurement of the  $^{41}\text{K}/^{39}\text{K}$  ratio, it has also been recognized its sensitivity to non-spectral matrix effects.<sup>9</sup> In the present study, we have evaluated the non-spectral matrix effects of Ca and Na with a K-normalized ratio ranging from 1 to 15% and compared the results with the literature values (Fig. 4).

The results show that Ca, Na and Mg interferences produce very little deviation of the  $\delta^{41}\text{K}$  value, except for Na with a Na/K ratio of 15%. Using CC-MC-ICP-MS, the Ca interference is thought to be generated by the reaction between  $\text{Ca}^+$  and  $\text{H}_2$  to form interfering  $^{40}\text{CaH}^+$  on  $^{41}\text{K}^+$ , leading to artificially high  $\delta^{41}\text{K}$  values.<sup>13,14</sup> The present results are consistent with this speculation, because without adding  $\text{H}_2$ , the Ca interference remains minor even at a  $[\text{Ca}]/[\text{K}]$  ratio of 15% (Fig. 4A). This substantial insensitivity to non-spectral matrix effects most probably results from the new design of the introduction system that integrates the iCAP Qnova Series ICP-MS assembly. This system, the same as the iCAP-Q ICP-MS, integrates a free-running solid-state RF generator capable of eliminating capacitive grounding using a “balanced coil technology”, or virtual grounding. Virtual grounding is achieved by applying RF potential to both ends of the coil with a  $180^\circ$  phase shift. This creates a virtual ground at the centre of the coil, which greatly improves plasma stability

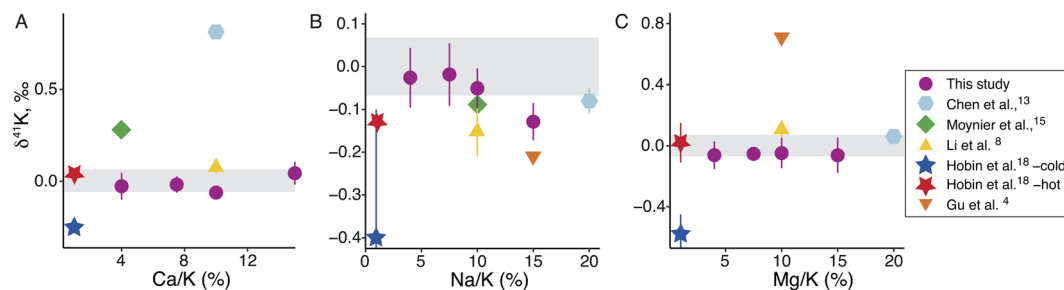


Fig. 4 Effect of matrix effects on the  $\delta^{41}\text{K}$  value of the sample as a function of the analyte K-normalized ratio (%) for Ca (A), Na (B), and Mg (C). The highest [Ca]/[K], [Na]/[K], and [Mg]/[K] value, which has been determined graphically, is indicated for each contribution of the literature. The gray area represents  $\pm 0.07\text{‰}$  from SRM-3141a. The error bars are  $\pm 2\text{SD}$ .

and dramatically reduces the formation of doubly charged ions, ion low energy spread and very low contamination of the sample due to degradation of the sampler cone.

### The $^{41}\text{K}/^{39}\text{K}$ ratio in geological and biological reference materials

The observed weak sensibility of the Neoma MC-ICP-MS to non-spectral matrix effects prompted us to develop a simple one step chemical purification of K based on Mg purification.<sup>20</sup> However, a single purification step was insufficient for Mg-rich basalts, as these materials provoke unstable sample-standard bracketing measurements (see the Methods).

The K content of two procedural blanks varies from 24 to 35 ng thus representing a negligible contribution ( $\sim 0.003\%$ ) relative to the K present in  $\sim 2$  mg of geological ([K]  $\sim 0.4\%$  wt) or biological ([K]  $\sim 0.1\%$  wt) samples. The repeatability (or short-term external precision<sup>24</sup>) was evaluated by repeated analyses of the SRM-3141a solution at 0.25, 0.5 and 1 mg L<sup>-1</sup>, which gives a value of 0.06‰ (2SD,  $n = 55$ ) regardless of the concentration. The intermediate precision, or long-term external reproducibility, that includes inconsistency of sample processing and  $^{41}\text{K}/^{39}\text{K}$  ratio measurements, was evaluated from the uncertainties measured on the reference materials, which gives a value of 0.07‰ (2SD,  $n = 12$ ).

The reference material measured in the present study agrees well with that in the literature. The granite GA and the basalts BCR-1 and BHVO-2 give a  $\delta^{41}\text{K}$  value of  $-0.50\text{‰}$ ,  $-0.40\text{‰}$  and  $-0.40\text{‰}$ , respectively. IAPSO seawater gives a  $\delta^{41}\text{K}$  value of  $0.03 \pm 0.02\text{‰}$  (2SD,  $n = 2$ ), slightly lower than the accepted average seawater  $\delta^{41}\text{K}$  value of  $0.12 \pm 0.07\text{‰}$  (2SD,  $n = 46$ ),<sup>25</sup> but still in the range of isotopic variability. The tuna fish ERM-CE 464 reference material yields a  $\delta^{41}\text{K}$  value of  $0.38 \pm 0.01\text{‰}$  (2SD,  $n = 2$ ), consistent with the value of  $0.31 \pm 0.05\text{‰}$  (2SD,  $n = 2$ ) reported by Moynier *et al.*,<sup>15</sup> and the lobster hepatopancreas TORT-3 reference material gives a  $\delta^{41}\text{K}$  value of  $-0.29 \pm 0.03\text{‰}$  (2SD,  $n = 2$ ), consistent with the value of  $-0.31 \pm 0.03\text{‰}$  (2SD,  $n = 3$ ) reported by Hobin *et al.*<sup>18</sup> The  $\delta^{41}\text{K}$  value of the DORM-4 fish protein is  $-0.24 \pm 0.03\text{‰}$  (2SD,  $n = 2$ ). The bovine liver SRM-1577c gives a  $\delta^{41}\text{K}$  value of  $0.15 \pm 0.004\text{‰}$  (2SD,  $n = 2$ ), different from the bovine liver ERM-BB185 reported by Moynier *et al.*<sup>15</sup> at  $-0.22 \pm 0.03\text{‰}$  (2SD,  $n = 2$ ), showing a metabolic influence of the hepatic K isotope composition that remains to

be elucidated. The significant effect of biological activity on the bodily K isotope composition is also highlighted by the very negative  $\delta^{41}\text{K}$  value ( $-2.11 \pm 0.15\text{‰}$ ) of the fetal bovine serum. The whole milk BCR-380 is at  $0.09\text{‰}$ , the green beans BCR-383 at  $-0.79\text{‰}$ , and the rye grass ERM-CD 281 at  $-0.23\text{‰}$ . The  $\delta^{41}\text{K}$  values of the reference materials are given in Table S2† and shown in Fig. 5 with literature values (also synthesized in Table S2†)<sup>31</sup> for marine and terrestrial plant and animal samples.

The resulting K isotope systematics reveals a protracted intra-individual variability, ranging from  $\sim -2\text{‰}$  (fetal bovine serum, this study) to  $\sim +1\text{‰}$  (bovine muscle ERM-BB184 (ref. 15)), therefore encompassing the terrestrial isotopic range.<sup>6</sup> Such a wide range of  $\delta^{41}\text{K}$  values has already been acknowledged<sup>14,18</sup> and highlights the potential use of K isotopes to study K metabolism in health and disease. At this stage, the present compilation of  $\delta^{41}\text{K}$  values does not support any trophic effect or difference between the marine and terrestrial realms, but this would require dedicated studies focusing on restricted food chains.

### The $^{41}\text{K}/^{39}\text{K}$ ratio in cancer and control blood samples

Using a Dempster-type mass spectrograph<sup>1,2</sup> developed by A. K. Brewer in the late 1930s, tentative measurements of the  $^{41}\text{K}/^{39}\text{K}$  ratio in solid tumors and adjacent normal tissues were

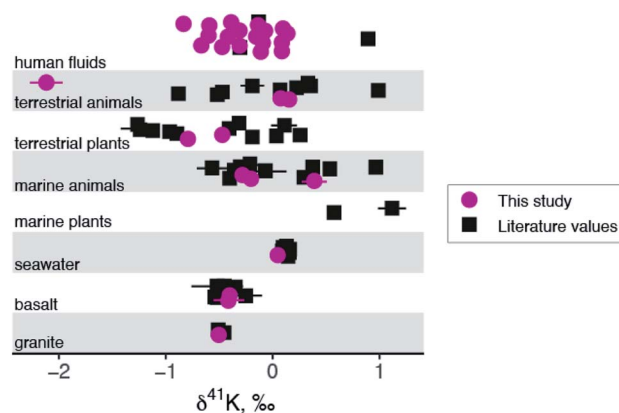


Fig. 5  $\delta^{41}\text{K}$  values measured in the present study compared to literature values. A focus has been made on the marine and terrestrial plant and animal K isotopic variability.

attempted,<sup>26,27</sup> revealing a measurable decrease of <sup>41</sup>K in cancerous compared to control tissues. Following lines of evidence made with Cu that the isotope composition can be fractionated in solid tumors relative to normal tissue,<sup>28</sup> which is traceable in blood<sup>29,30</sup> and has diagnostic or prognostic utility, we have measured the serum  $\delta^{41}\text{K}$  value of newly diagnosed acute myeloid leukemia patients and compared the results with age-matched control participants. The results show a non-significant difference ( $P$  value = 0.70 and  $n = 19$ , Table S2†) between patients and controls. However, the suspected <sup>41</sup>K-depleted signature of solid tumors relative to normal tissue made almost 90 years ago is worth revisiting using modern MC-ICP-MS instrumentation.

## Conclusion

We report K isotopic data measured using a Thermo Scientific Neoma MC-ICP-MS with the XHR mode for 12 geological and biological reference materials and human blood samples. We show that this instrument displays substantial robustness to non-spectral matrix effects and medium mismatches between samples and standards, which allows the development of a simple single-step K purification prior to isotopic measurements. The resulting short-term and long-term precision is 0.06‰ and 0.07‰, respectively, and comparable with other techniques. This instrumental robustness remains to be challenged with the pre-cell mass filter and hexapole collision/reaction cell upgrade.

## Conflicts of interest

There are no conflicts to declare.

## Acknowledgements

This study was performed using the INSU/CNRS MC-ICP-MS national facility at ENS-Lyon. We thank two anonymous reviewers for their helpful insights during the review process and the ThermoFischer Scientific company for their support and training during the installation of the Neoma instrument.

## References

- 1 A. K. Brewer, *J. Am. Chem. Soc.*, 1936, **58**, 365–370.
- 2 A. K. Brewer, *J. Am. Chem. Soc.*, 1937, **59**, 869–872.
- 3 H. Chen, Z. Tian, B. Tuller-Ross, R. L. Korotev and K. Wang, *J. Anal. At. Spectrom.*, 2019, **34**, 160–171.
- 4 H.-O. Gu and H. Sun, *J. Anal. At. Spectrom.*, 2021, **36**, 2545–2552.
- 5 Y. Hu, X.-Y. Chen, Y.-K. Xu and F.-Z. Teng, *Chem. Geol.*, 2018, **493**, 100–108.
- 6 L. E. Morgan, D. P. S. Ramos, B. Davidheiser-Kroll, J. Faithfull, N. S. Lloyd, R. M. Ellam and J. A. Higgins, *J. Anal. At. Spectrom.*, 2018, **33**, 175–186.
- 7 Y.-K. Xu, Y. Hu, X.-Y. Chen, T.-Y. Huang, R. S. Sletten, D. Zhu and F.-Z. Teng, *Chem. Geol.*, 2019, **513**, 101–107.
- 8 X. Li, G. Han, Q. Zhang and Z. Miao, *J. Anal. At. Spectrom.*, 2020, **35**, 1330–1339.
- 9 S. J. Jiang, R. S. Houk and M. A. Stevens, *Anal. Chem.*, 1988, **60**, 1217–1221.
- 10 F. M. Richter, E. Bruce Watson, M. Chaussidon, R. Mendybaev, J. N. Christensen and L. Qiu, *Geochim. Cosmochim. Acta*, 2014, **138**, 136–145.
- 11 W. Li, B. L. Beard and S. Li, *J. Anal. At. Spectrom.*, 2016, **31**, 1023–1029.
- 12 K. Wang and S. B. Jacobsen, *Geochim. Cosmochim. Acta*, 2016, **178**, 223–232.
- 13 H. Chen, N. J. Saunders, M. Jerram and A. N. Halliday, *Chem. Geol.*, 2021, **578**, 120281.
- 14 F. Moynier, Y. Hu, W. Dai, E. Kubik, B. Mahan and J. Moureau, *J. Anal. At. Spectrom.*, 2021, **36**, 2444–2448.
- 15 F. Moynier, Y. Hu, K. Wang, Y. Zhao, Y. Gérard, Z. Deng, J. Moureau, W. Li, J. I. Simon and F.-Z. Teng, *Chem. Geol.*, 2021, **571**, 120144.
- 16 D. Bevan, C. D. Coath, J. Lewis, J. Schwieters, N. Lloyd, G. Craig, H. Wehrs and T. Elliott, *J. Anal. At. Spectrom.*, 2021, **36**, 917–931.
- 17 G. Craig, H. Wehrs, D. G. Bevan, M. Pfeifer, J. Lewis, C. D. Coath, T. Elliott, C. Huang, N. S. Lloyd and J. B. Schwieters, *Anal. Chem.*, 2021, **93**, 10519–10527.
- 18 K. Hobin, M. Costas Rodríguez and F. Vanhaecke, *Anal. Chem.*, 2021, **93**, 8881–8888.
- 19 M. Ohanian, P. Telouk, S. Kornblau, F. Albarede, P. Ruvolo, R. S. S. Tidwell, A. Plesa, R. Kanagal-Shamanna, E.-L. Matera, J. Cortes, A. Carson and C. Dumontet, *Am. J. Hematol.*, 2020, **95**, 422–434.
- 20 S. Le Goff, E. Albalat, A. Dosseto, J.-P. Godin and V. Balter, *Rapid Commun. Mass Spectrom.*, 2021, **35**, e9074.
- 21 E. W. E. Strelow, F. Von S. Toerien and C. H. S. W. Weinert, *Anal. Chim. Acta*, 1970, **50**, 399–405.
- 22 N. Dauphas, A. Pourmand and F.-Z. Teng, *Chem. Geol.*, 2009, **267**, 175–184.
- 23 S. H. Tan and G. Horlick, *J. Anal. At. Spectrom.*, 1987, **2**, 745–763.
- 24 A. Makishima, *Thermal Ionization Mass Spectrometry (TIMS): Silicate Digestion, Separation, Measurement*, Wiley-VCH Verlag, Weinheim, 2016.
- 25 K. Wang, H. G. Close, B. Tuller-Ross and H. Chen, *ACS Earth Space Chem.*, 2020, **4**, 1010–1017.
- 26 A. Lasnitski and A. K. Brewer, *Nature*, 1938, **142**, 538–539.
- 27 A. Lasnitski and A. K. Brewer, *Nature*, 1942, **149**, 357–358.
- 28 V. Balter, A. N. da Costa, V. P. Bondanese, K. Jaouen, A. Lamboux, S. Sangrajrang, N. Vincent, F. Fourel, P. Télouk, M. Gigou, C. Lécuyer, P. Srivatanakul, C. Bréchet, F. Albarède and P. Hainaut, *Proc. Natl. Acad. Sci. U.S.A.*, 2015, **112**, 982–985.
- 29 P. Télouk, A. Puisieux, T. Fujii, V. Balter, V. P. Bondanese, A.-P. Morel, G. Clapison, A. Lamboux and F. Albarede, *Met. Integ. Biometal Sci.*, 2015, **7**, 299–308.
- 30 L. Lobo, M. Costas-Rodríguez, J. C. de Vicente, R. Pereiro, F. Vanhaecke and A. Sanz-Medel, *Talanta*, 2017, **165**, 92–97.
- 31 W. Li, *Acta Geochim.*, 2017, **36**, 374–378.